Surface degradation of superconducting $YBa_2Cu_3O_{7-\delta}$ thin films

S. E. Russek, S. C. Sanders, A. Roshko, and J. W. Ekin
Electromagnetic Technology Division, National Institute of Standards and Technology, Boulder, Colorado 80303

The surface degradation of c-axis oriented $YBa_2Cu_3O_{7-\delta}$ thin films due to air, CO_2, N_2, O_2, and vacuum exposure has been studied with reflection high-energy electron diffraction (RHEED), scanning tunneling microscopy, and contact resistivity measurements. The formation of an amorphous surface reaction layer upon exposure to air and CO_2 is monitored with RHEED and correlated with an increase in contact resistivity. The contact resistivity of samples exposed to air increases with time t as $\rho_c = (1.0 \times 10^{-7} \ \Omega \ cm^2)e^{\sqrt{t/640 \ min}}$. Surfaces exposed to CO_2 show a similar degradation while surfaces exposed to N_2 showed a slightly different degradation mechanism. Vacuum exposed surfaces how little increase in contact resistivity, indicating no long-term surface oxygen loss.

Understanding the nature of $YBa_2Cu_3O_{7-\delta}$ (YBCO) surfaces and how they degrade in different environments is crucial to the development of YBCO contact technologies[1] and superconductor-normal metal-superconductor proximity devices.[2] In this letter, we investigate the effects of exposure to air, CO_2, N_2, O_2, and vacuum on YBCO surfaces. We correlate the growth of an amorphous surface reaction layer for exposure to air, CO_2 and N_2, as seen by reflection high-energy electron diffraction (RHEED), with Ag-YBCO contact resistivity. We find that the contact resistivity, after exposure to air, increases exponentially with the square root of time. Further, exposure to N_2 has a different degradation mechanism than that to air or CO_2 and some surface degradation occurs during *in situ* processing.

Early x-ray diffraction, x-ray photoelectron spectroscopy (XPS), and Auger electron spectroscopy[3-5] work has shown that upon exposure to air, a YBCO surface will react to form $Ba(OH)_2$ and $BaCO_3$. More recent XPS work of Behner *et al.*[6] has quantified the thickness of the reaction layer, showing that the reaction layer thickness d increases with the square root of time as $d = 0.013(nm/\sqrt{min})\sqrt{t}$. High-resolution transmission electron microscopy (TEM) studies by Gong *et al.*[7,8] have shown the presence of a reaction layer for c-axis YBCO-Ag contacts when the Ag is deposited *in situ* at room temperature. They have observed no reaction layer for similarly fabricated a-axis YBCO-Ag contacts indicating that the chemical reactivity of YBCO is anisotropic. The results presented in this paper support some of the conclusions reached in these earlier studies and provide detailed time dependence of the YBCO-Ag contact resistivity after exposure to various types of environments.

The YBCO thin films for our experiments were fabricated by laser ablation using a KrF excimer laser. All films were grown on (100) MgO and (100) $LaAlO_3$ substrates with the following growth parameters: substrate temperature $=730 \ °C$, O_2 pressure during growth$=26.7$ Pa (200 mTorr), growth rate$=0.03$ nm/pulse at 10 Hz, and incident laser fluence$=2.1 \ J/cm^2$. The YBCO thickness was kept constant at 200 nm. After the YBCO growth, the films were cooled to room temperature in 15 min to 60 min in 26.7 kPa (200 Torr) of oxygen. The system was then evacuated and the films

were characterized with RHEED using an incident electron energy of 20 keV and an incident angle of 1°. Some of the films were then exposed, for times ranging from 10 to 10 000 min, to air, CO_2, N_2, O_2, or vacuum, in the system or the system load lock. The exposed surfaces were recharacterized with RHEED and then a 250-nm Ag contact layer was thermally deposited at room temperature. Similar contacts were formed on nonexposed (*in situ*) films. Finally, the films were patterned to form contact resistivity test structures, with contact dimensions of 2, 4, 8, and 16 μm on a side. The measured contact resistances scaled well with contact area. The zero-resistance transition temperatures (T_{c0}) ranged from 86 to 89 K, and the critical current densities at 76 K ranged from 1 to $4\times10^6 \ A/cm^2$.

Figure 1 shows a RHEED pattern of as-deposited YBCO film on MgO and a scanning tunneling microscopy (STM) image of the same film. The films on MgO have a spiral growth morphology with a spiral density of $\sim3\times10^9 \ cm^{-2}$ and have a ratio of a-axis to c-axis exposed area of 0.04. The

FIG. 1. RHEED pattern of as-deposited YBCO film deposited on MgO along the (100) direction (inset) and (b) STM image of the same film. The average ledge width (the distances between growth steps) is ~30 nm.
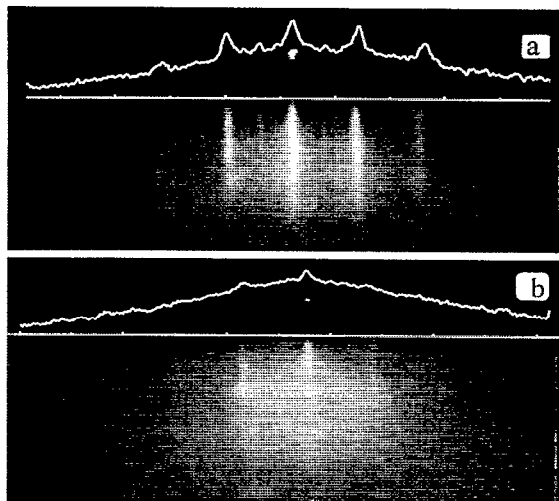
FIG. 2. (a) RHEED pattern and line scan of as-deposited YBCO film along the YBCO and MgO (110) direction. (b) RHEED pattern and line scan of the same film after 1000-min air exposure.

FIG. 3. Contact resistivity of Ag-YBCO interfaces at 4 K as a function of exposure time for air, CO_2, N_2, O_2, and vacuum exposure. The contact resistivity values are the average contact resistivity of the various size devices on each chip. The vertical error bars represent the rms spread in the contact resistivity values for the devices on each chip. The exposure times for the in situ contacts are calculated effective exposure times.

films grown on $LaAlO_3$ have an island growth morphology with a similar ratio of a-axis to c-axis exposed area. The RHEED pattern shows streaks, indicating a crystalline surface with an in-plane lattice constant of 0.38 ± 0.01 nm, consistent with the lattice constant of bulk YBCO. The streaks indicate that the diffraction pattern arises from two-dimensional surface scattering, and the width of the streaks yields an effective scattering coherence length of 3–5 nm. This length is less than the average ledge width of ~30 nm, and hence the diffraction pattern is sampling smooth regions on a scale much less than the average size of the spirals or islands. This explains why RHEED patterns of YBCO films are fairly insensitive to film topography. While the RHEED pattern in Fig. 1 does not show any signs of surface reconstruction, often additional streaks are observed as seen in Fig. 2(a). The faint intermediate streaks indicate a 2×2 surface reconstruction. Reconstructed YBCO surfaces have been seen in low-energy electron diffraction (LEED) and RHEED studies[8] and it has been suggested that the reconstruction is due to surface oxygen loss. We have not, however, found any correlation between the presence of the reconstruction peaks and the way the YBCO film was grown, nor any correlation with the cooldown procedure and time before RHEED imaging. A more comprehensive characterization of these films by RHEED and STM is presented in Ref. 9.

RHEED images of the YBCO surface before and after air exposure are shown in Figs. 2(a) and 2(b). The diffracted peak height decreases while the diffuse background intensity increases with air exposure. This is a clear signature that an amorphous reaction layer is forming on the surface. The ratio of diffracted peak intensity to the intensity of the diffuse background decreases monotonically with time. The diffraction peaks can be seen for up to one week of air exposure, after which they disappear into the diffuse background.

The 4-K contact resistivity of the air-exposed samples as a function of exposure times is shown in Fig. 3 (all air ex-
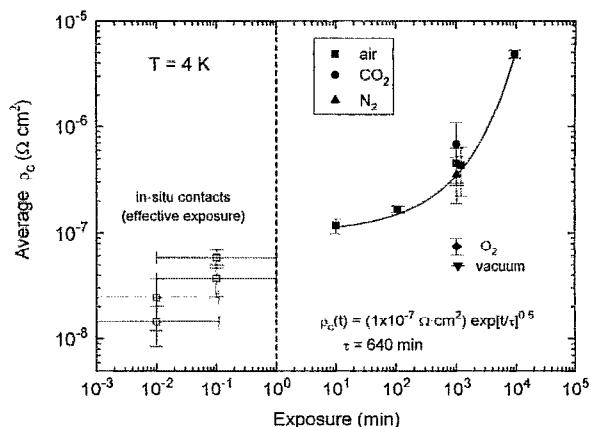
posures were done at $25\pm5\%$ relative humidity). The air exposed data can be fit by an exponential of the form $\rho_c = (1.0 \times 10^{-7} \ \Omega \ \mathrm{cm}^2)e^{\sqrt{t/640 \ \mathrm{min}}}$. The square-root dependence on the exposure time suggests that the contact resistivity is exponentially dependent on a barrier thickness d, which increases through a diffusion-limited chemical reaction. This result is in agreement with the XPS studies of Behner et al.[6] The exponential dependence of the contact resistivity on time indicates that the electron transport occurs through a tunneling mechanism. Other mechanisms leading to a power-law increase of the contact resistivity, such as loss of contact area due to a reaction propagating inward from the growth steps or other nucleation sites (such as screw dislocations), can be ruled out.

Figure 3 shows for comparison the contact resistivities of several in situ contact chips. The in situ contact resistivities are in the low $10^{-8} \ \Omega \ \mathrm{cm}^2$ range. These values are slightly higher than those obtained in an earlier study[10] on sputtered YBCO films, which had slightly different electrical properties and surface morphologies. The in situ contact resistivities are plotted versus an effective exposure time which normalizes the in situ exposure to atmospheric exposure assuming the surface degradation arises only from water vapor. Different effective exposure times were obtained by varying the cooldown time and the residual gas partial pressure during cooldown. When the effective exposure time was reduced, the contact resistivities decreased slightly, indicating that some surface reaction is occurring in the chamber during cooldown. This result is consistent with the TEM studies of Gong et al.,[8] who observed a 2-nm reaction layer between c-axis YBCO and Ag for in situ contacts deposited at room temperature.

The fit to the contact resistivity for the samples exposed to air does not extrapolate to the values for the in situ contacts. This suggests that there are two degradation processes with different time constants. The contaminant gases in the chamber have a different composition than air and may have a slower reaction rate. Alternatively, as suggested by Gong
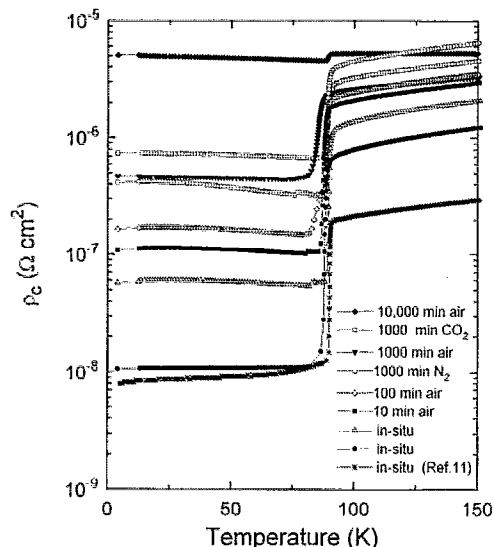
Russek et al.

FIG. 4. Temperature dependence of Ag-YBCO contact resistivity for interfaces with different types of surface preparation. Above T_c the device resistance is the sum of the YBCO spreading resistance and the contact resistance, while below T_c the resistance is just the contact resistance.

et al., there may be different reaction rates for the crystal faces parallel and perpendicular to the c axis. One crystalline face may rapidly degrade while the other degrades slowly, leading to the long-time decrease in the surface conductance seen in Fig. 3. An anisotropic surface reaction, after exposure to air, is suggested by STM data of Moreland et al.[11] that show surface conductance peaks near the growth step edges.

Figure 3 also shows the contact resistivity of films exposed for 1000 min to CO_2, N_2, O_2, and vacuum. The films exposed to CO_2 show RHEED and contact resistivity data similar to samples exposed to air. The films exposed to N_2 did not show as severely degraded RHEED patterns as those exposed to air or CO_2. The ratio of the diffracted peak height to the diffuse background for the 1000-min N_2 exposure was larger than that for the 100-min air exposure. Surprisingly, the contact resistivity of samples exposed to N_2 increased nearly as fast as those exposed to air. These data indicate that a different type of reaction mechanism occurs with N_2. Reaction of YBCO surfaces with N_2 has been seen with LEED by Ohara et al.[12] These studies used much lower N_2 doses, and the analysis with LEED was more surface sensitive. The sample exposed to oxygen did not show any noticeable degradation of the RHEED image and showed a slight increase in contact resistivity consistent with a continued surface reaction with impurity gases present in the chamber. The sample exposed to vacuum showed little increase in contact resistivity indicating that, as expected, there was no further surface reaction. This result also shows that there is no long-term surface oxygen loss when the films are stored in vacuum. A surface oxygen loss at room temperature has been observed by several groups;[13,14] however, this oxygen loss must occur quickly and be self limiting.

The temperature dependencies of the contact resistivities for samples exposed to air, CO_2, and N_2 are shown in Fig. 4. The contact resistivity below 90 K decreases slightly with decreasing temperature for devices with lower contact resistivity, increases slightly for devices with higher contact resistivity, and has a slight peak for devices with intermediate contact resistivity. The change in contact resistivity is typically 5%–10% between 77 and 4 K. The samples exposed to N_2 show a somewhat anomalous 20% increase in contact resistivity from 77 to 4 K. The weak temperature dependence for all devices, including the in situ contacts, supports a tunneling model for interface transport.

In summary, the contact resistivity, after exposure to air, increases with time t as $\rho_c = (1.0 \times 10^{-7}\ \Omega\ cm^{-2})e^{\sqrt{t/640\ \text{min}}}$. CO_2 exposure shows a degradation in the RHEED pattern and contact resistivity similar to air exposure. N_2 exposure, however, shows a somewhat different degradation mechanism in which the crystallinity of the c-axis faces does not degrade as fast as that for air exposure while the contact resistivity increases at a similar rate. The vacuum exposure experiments indicate that there is no long-term surface oxygen loss when YBCO films are stored in a vacuum. The exponential increase in contact resistivity with time and the flat temperature dependence are strong indications that the conduction occurs through a tunneling process. The change in contact resistivity for different in situ processing conditions indicates that some surface degradation occurs during in situ processing.

[1] J. W. Ekin, in Processing and Properties of High-T_c Superconductors, edited by S. Jin (World Scientific, Singapore, 1993), p. 371.
[2] R. H. Ono, J. A. Beall, M. W. Cromar, T. E. Harvey, M. E. Johansson, C. D. Reintsema, and D. A. Rudman, Appl. Phys. Lett. 59, 1126 (1991).
[3] M. F. Yan, R. L. Barns, H. M. O'Brian, Jr., P. K. Gallagher, R. C. Sherwood, and S. Jin, Appl. Phys. Lett. 51, 532 (1987).
[4] C. C. Chang, M. S. Hedge, X. D. Wu, B. Dutta, A. Inam, T. Venkatesan, B. J. Wilkens, and J. B. Wachtman, Appl. Phys. Lett. 55, 1680 (1989).
[5] Temel H. Büyüklimanli and Joseph H. Simmons, Phys. Rev. B 44, 727 (1991).
[6] H. Behner, K. Rührnschopf, G. Wedler, and W. Rauch, Physica C 208, 419 (1993).
[7] Z. H. Gong, R. Fagerberg, F. Vassenden, J. K. Grepstad, and R. Høier, Appl. Phys. Lett. 60, 498 (1992).
[8] Z. H. Gong, F. Vassenden, R. Fagerberg, J. K. Grepstad, A. Bardal, and R. Høier, Appl. Phys. Lett. 63, 836 (1993).
[9] S. E. Russek, A. Roshko, S. C. Sanders, D. A. Rudman, J. W. Ekin, and J. Moreland, Mater. Res. Soc. Symp. Proc. 285, 305 (1993).
[10] J. W. Ekin, S. E. Russek, C. C. Clickner, and B. Jeanneret, Appl. Phys. Lett. 62, 369 (1993).
[11] J. Moreland, P. Rice, S. E. Russek, B. Jeanneret, A. Roshko, R. H. Ono, and D. A. Rudman, Appl. Phys. Lett. 59, 3039 (1991).
[12] T. Ohara, K. Sakuta, M. Kamishiro, and T. Kobayashi, Jpn. J. Appl. Phys. 30, L2085 (1991).
[13] H. Behner, W. Rauch, and E. Gornik, Appl. Phys. Lett. 61, 1465 (1992).
[14] R. S. List, A. J. Arko, Z. Fisk. S.-W. Cheong, S. D. Conradson, J. D. Thompson, C. B. Pierce, D. E. Peterson, R. J. Bartlett, N. D. Shinn, J. E. Schirber, B. W. Veal, A. P. Paulikas, and J. C. Campuzano, Phys. Rev. B 38, 11966 (1988).

Appl. Phys. Lett., Vol. 64, No. 26, 27 June 1994

Russek et al.   3651